

# Optomechanical cooling by STIRAP-assisted energy transfer – an alternative route towards the mechanical ground state

Bijita Sarma and Thomas Busch

Quantum Systems Unit, Okinawa Institute of Science and Technology Graduate University, Okinawa 904-0495, Japan

Jason Twamley

Centre for Engineered Quantum Systems, Department of Physics and Astronomy,  
Macquarie University, Sydney, New South Wales 2109, Australia

(Dated: December 21, 2024)

Standard optomechanical cooling methods ideally require weak coupling and cavity damping rates which enable the motional sidebands to be well resolved. If the coupling is too large then sideband-resolved cooling is unstable or the rotating wave approximation can become invalid. In this work we describe a protocol involving two driven optical cavities one of which is optomechanically coupled to a mechanical oscillator. We show that by modulating both the amplitudes and frequencies of optical drives one can execute a type of STIRAP transfer of occupation from the mechanical mode to a lossy auxiliary optical mode which results in cooling of the mechanical mode. We show how this protocol can outperform normal optomechanical sideband cooling in various regimes such as the strong coupling and the unresolved sideband limit.

**Introduction** — Mesoscopic mechanical resonators have recently garnered extensive theoretical and experimental research interest due to their potential uses in quantum information processing and quantum state engineering [1–3]. They exhibit high coupling efficiency to optical and microwave fields, and in the field of cavity optomechanics, nanomechanical resonators have been studied to generate entanglement between optical and mechanical modes, to facilitate state transfer between optical and microwave fields, etc. However, optomechanical resonators are always in contact with a thermal bath, which hampers the observation of many quantum effects and requires their cooling to the ground state. For this, conventional cavity cooling makes use of optomechanically enhanced damping due to radiation pressure coupling, where the norm is to drive an optomechanical cavity at the red sideband so that the cooling rate can be increased in comparison to the heating rate. In order to resolve the Stokes and anti-Stokes sidebands the cavity decay rate has typically to be much smaller than the mechanical frequency,  $\kappa \ll \omega_b$ . In this *resolved sideband regime* a variety of optomechanical cooling schemes exist, including ones based on cavity backaction cooling [4, 5], dissipative optomechanical coupling [6, 7], feedback cooling [8–12], quadratic coupling [13, 14], sideband cooling [15, 16], transient cooling [17, 18], cooling based on the quantum interference effect [19–21], and others. A few proposals for cooling in the unresolved-sideband regime have been developed as well, based on modulation of the cavity damping rate [22], using resonant intracavity optical gain [23] or squeezed light [24, 25], however, these are difficult to implement experimentally.

In this letter we propose a novel method to cool an optomechanical system based on adiabatic transfer of phonons into photons. Our model consists of an optomechanical system where a primary cavity is coupled to a

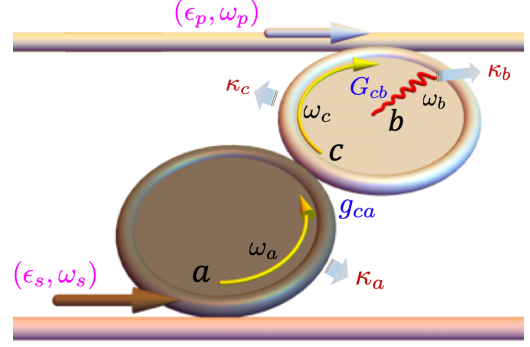


Figure 1. (Color online) Schematic cooling setup: a primary cavity, with mode  $c$ , and an auxiliary cavity, with mode  $a$ , are coupled at a fixed rate  $g_{ca}$ . At the same time the primary cavity mode  $c$  is also optomechanically coupled to a mechanical mode  $b$ , at rate  $G_{cb}$ , whose strength is modulated via an optical drive on the primary cavity. By modulating both the amplitudes and frequencies of optical drives applied to the auxiliary  $(\epsilon_s, \omega_s)$ , and primary  $(\epsilon_p, \omega_p)$  optical cavities, occupation can be transferred from the mechanical mode to the auxiliary cavity mode, thus cooling the mechanics.

mechanical resonator, and also to an auxiliary optical cavity. We consider that both the optical cavities are driven and we show that by modulating the amplitudes and frequencies of these drives we can transfer phonons from the mechanical resonator to the auxiliary cavity mode without populating the primary cavity. We use a technique similar to Stimulated Raman Adiabatic Passage (STIRAP) to drain the phononic excitations to the auxiliary lossy optical cavity and by repeatedly iterating the pulses sequence, we show that it is possible to cool the mechanical mode down to the ground state. The advantage of our method is that it operates over a much broader range of conditions than what can be accommodated using standard sideband cooling methods.

**Model** — To study the cooling of a mechanical resonator mode into the ground state we consider a system

consisting of a primary optomechanical cavity coupled to an auxiliary optical cavity, as shown in Fig. 1. The Hamiltonian of the system is given by ( $\hbar = 1$ )

$$H_0 = \omega_a a^\dagger a + \omega_c c^\dagger c + \omega_b b^\dagger b + g_{ca}(a^\dagger c + c^\dagger a) + g_{cb}c^\dagger c(b + b^\dagger) + i(\varepsilon_s a^\dagger e^{-i\omega_s t} - \varepsilon_s^* a e^{i\omega_s t}) + i(\varepsilon_p c^\dagger e^{-i\omega_p t} - \varepsilon_p^* c e^{i\omega_p t}), \quad (1)$$

where  $a(a^\dagger)$ ,  $c(c^\dagger)$  and  $b(b^\dagger)$  are the annihilation (creation) operators of the auxiliary cavity mode, primary cavity mode and mechanical mode respectively. In addition,  $g_{ca}$  and  $g_{cb}$  are the single excitation coupling rates of the cavity-cavity and cavity-phonon interaction. The last two terms describe the external driving of the cavity modes, where,  $\varepsilon_s(t)$  and  $\varepsilon_p(t)$  are the amplitudes of the drives with frequencies  $\omega_s(t)$  and  $\omega_p(t)$ , applied on the optical modes  $a$  and  $c$ , respectively. Moving to a doubly-rotating frame via the transformation,  $R = \exp[i(\omega_s(t) a^\dagger a + \omega_p(t) c^\dagger c)t]$ , with  $H = RH_0 R^\dagger + i\frac{\partial R}{\partial t} R^\dagger$ , and neglecting terms linear in  $\dot{\omega}_s$ ,  $\dot{\omega}_p$ , the transformed Hamiltonian of the system can be written as

$$H = \Delta_a a^\dagger a + \Delta_c c^\dagger c + \omega_b b^\dagger b + g_{ca}(a^\dagger c + c^\dagger a) + g_{cb}c^\dagger c(b + b^\dagger) + i(\varepsilon_s a^\dagger - \varepsilon_s^* a) + i(\varepsilon_p c^\dagger - \varepsilon_p^* c) \quad (2)$$

where  $\Delta_a(t) = \omega_a - \omega_s(t)$  and  $\Delta_c(t) = \omega_c - \omega_p(t)$  are the cavity detunings. The dynamical evolution of the system operators can be described by the Langevin equations

$$\begin{aligned} \dot{a} &= (-i\Delta_a - \kappa_a)a - ig_{ca}c + \varepsilon_s + \sqrt{2\kappa_a}a_{\text{in}}, \\ \dot{b} &= (-i\omega_b - \kappa_b)b - ig_{cb}c^\dagger c + \sqrt{2\kappa_b}b_{\text{in}}, \\ \dot{c} &= (-i\Delta_c - \kappa_c)c - ig_{ca}a - ig_{cb}c(b + b^\dagger) + \varepsilon_p + \sqrt{2\kappa_c}c_{\text{in}}, \end{aligned} \quad (3)$$

where  $\kappa_a$ ,  $\kappa_c$  and  $\kappa_b$  are the losses of the cavity modes and the mechanical mode, respectively. The  $a_{\text{in}}$ ,  $c_{\text{in}}$  and  $b_{\text{in}}$  are the noise operators with zero mean values and correlation functions given by  $\langle A_{\text{in}}(t)A_{\text{in}}^\dagger(t') \rangle = (\bar{n}_A + 1)\delta(t - t')$ ,  $\langle A_{\text{in}}^\dagger(t)A_{\text{in}}(t') \rangle = \bar{n}_A\delta(t - t')$ , and where  $\bar{n}_A = (e^{\hbar\omega_A/k_B T_{\text{bath}}} - 1)^{-1}$ , with  $A = \{a, b, c\}$ , are the mean thermal occupations of the modes. Here  $T_{\text{bath}}$  is the common bath temperature and  $k_B$  is the Boltzmann constant. For strong driving, each Heisenberg operator can be expressed as a sum of its steady-state mean value and the quantum fluctuation, i.e.,  $a = \alpha + a_1$ ,  $b = \beta + b_1$  and  $c = \eta + c_1$ , where  $\alpha$ ,  $\beta$ ,  $\eta$  are the classical mean field values of the modes and  $a_1$ ,  $b_1$ ,  $c_1$  are the corresponding quantum fluctuation operators. From the quantum Langevin equations the linearized Hamiltonian can be written in the form (see supplementary material)

$$H_{\text{lin}} = \Delta_a a_1^\dagger a_1 + \Delta_c c_1^\dagger c_1 + \omega_b b_1^\dagger b_1 + G_{cb}(c_1 + c_1^\dagger)(b_1 + b_1^\dagger) + g_{ca}(c_1^\dagger a_1 + c_1 a_1^\dagger), \quad (4)$$

where  $G_{cb} = \eta g_{cb}$  is the coherent-driving-enhanced linearized optomechanical coupling strength. Since  $\eta$  is proportional to the amplitude of the driving field,  $\varepsilon_p$ , one can modulate  $G_{cb}$  via the external optical drive on  $\hat{c}$ . However, it is to be noted that the cavity-cavity coupling  $g_{ca}$

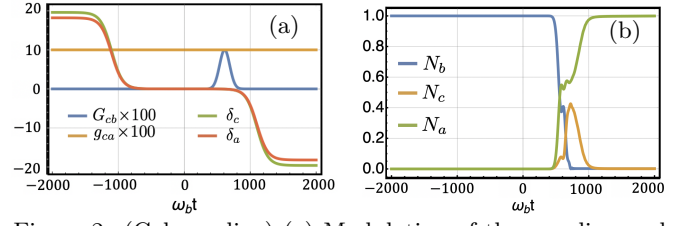


Figure 2. (Color online) (a) Modulation of the coupling and detuning pulses for the case when  $\Omega_0/\omega_b = 0.1$ . Here  $\delta_a$ ,  $\delta_c$  are the cavity detunings and  $G_{cb}$ ,  $g_{ca}$  are the coupling amplitudes in units of  $\omega_b$ . (b) Unitary time evolution of the modal populations using the pulses shown in (a),  $(N_b, N_c, N_a)$  are the mechanical, primary and auxiliary cavity mode occupations, where initially  $(N_b, N_a, N_c) = (1, 0, 0)$ . The pulse parameters used are shown in Table I.

cannot be modulated using such a technique and in what follows we will assume that we can time-modulate  $G_{cb}(t)$ , while  $g_{ca}$  is constant in time.

Transforming the Hamiltonian now to an interaction picture with  $U = \exp[-i\omega_b(a_1^\dagger a_1 + c_1^\dagger c_1 + b_1^\dagger b_1)t]$ , yields  $H = UH_{\text{lin}}U^\dagger$ , where

$$H = \delta_a(t)a_1^\dagger a_1 + \delta_c(t)c_1^\dagger c_1 + G_{cb}(t)\left(c_1^\dagger b_1 + c_1 b_1^\dagger + e^{-2i\omega_b t}c_1 b_1 + e^{2i\omega_b t}c_1^\dagger b_1^\dagger\right) + g_{ca}(c_1^\dagger a_1 + c_1 a_1^\dagger). \quad (5)$$

Here  $\delta_a(t) = \Delta_a(t) - \omega_b$  and  $\delta_c(t) = \Delta_c(t) - \omega_b$  are time-dependent detunings. One can see that the detunings are varied by tuning the frequencies of the input drives while the optomechanical coupling is varied by tuning the primary cavity drive amplitude. Using these time-dependent modulations we now seek to apply a STIRAP-like protocol to effectively transfer the phonon population to the auxiliary cavity mode. We also note that in most of our analysis below we will *not* make the RWA and the counter rotating terms in the Hamiltonian play an important role particularly when  $|G_{cb}|/\omega_b \ll 1$ .

**Population transfer protocol** — In conventional three-level atomic systems population can be transferred using a Stimulated Raman Adiabatic Passage (STIRAP) protocol. This relies on the fact that at two-photon resonance an instantaneous eigenvector with zero eigenvalue exists, which is a superposition of the initial and target states and which is called the *dark-state*. If the population can be confined to this state during the transfer process, a so-called ‘counter-intuitive’ modulation of the coupling strengths can be used to achieve a high fidelity transfer between the initial and the final state. However, this conventional STIRAP method cannot be straightforwardly applied to our system, as the cavity-cavity coupling,  $g_{ca}$  cannot be modulated in a time-dependent manner. In what follows we therefore use an alternate method which allows population transfer from the mechanical mode to the auxiliary cavity mode by modulating the detunings instead [26], and show how it allows us to cool the me-

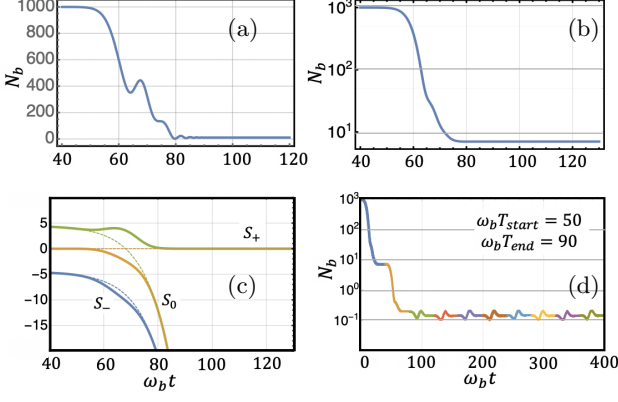


Figure 3. (Color online) Phonon cooling with and without coupling to thermal baths: (a) Evolution of phonon occupancy in the mechanical resonator,  $N_b(t)$ , while applying the complete transfer pulse (6)-(8), with  $(N_b, N_a, N_c) = (10^3, 0, 0)$  initially. This is obtained by solving the Master equation without considering any damping; (b) Evolution of  $N_b(t)$  after including damping in the system, with  $(\kappa_c, \kappa_a)/\omega_b = (0.5, 2.0)$ , and  $Q_b = 10^7$ , solved using the Master equation approach with initial values  $(N_b, N_a, N_c) = (10^3, 0, 0)$ ; (c) Solid (dashed) lines show the eigenvalues of the time-dependent Hamiltonian with (without) the pump coupling applied, showing the creation of a gap between  $S_+$  and  $S_0$ . (d)  $N_b(t)$ , when using a truncated pulse ( $\omega_b T_{start} = 0.5$  to  $\omega_b T_{end} = 0.9$ ), which encloses the gap and repeating it 10 times, indicated by different colours used. Parameters for all simulations shown are in Table I, and we note that here we have considered  $\Omega_0/\omega_b = 0.9$ , i.e. we are in the strong coupling regime where the RWA is no longer valid.

chanical resonator to the ground state.

For this we write the static optical cavity-cavity coupling, which is traditionally known as the ‘Stokes’ coupling, as  $g_{ca} \equiv \Omega_s/2 = \Omega_0/2$  and set the time dependent optomechanical coupling  $G_{cb}(t) \equiv \Omega_p/2$ , known as the ‘Pump coupling’, to be the Gaussian

$$\Omega_p(t) = \Omega_0 e^{-(\frac{t-t_c}{T})^2}, \quad (6)$$

centered at time  $t_c$ , with width  $T$ , and amplitude  $\Omega_0$ . We also apply detunings chosen as

$$\begin{aligned} \delta_c(t) &= \kappa_\delta \delta_s(t), \\ \delta_a(t) &= (\kappa_\delta - 1) \delta_s(t), \end{aligned} \quad (7)$$

where

$$\delta_s(t) = h_\delta \Omega_0 \left[ \tanh\left(\frac{t-\tau}{\tau_{ch}}\right) + \tanh\left(\frac{t+\tau}{\tau_{ch}}\right) \right], \quad (8)$$

and we will seek values of the parameters  $(\kappa_\delta, h_\delta, \tau, \tau_{ch})$ , to obtain the best cooling of the  $b$ -mode for a given strength of driving  $\Omega_0/\omega_b$ . The pulse shapes are shown in Fig. 2(a). Here, the parameter  $\Omega_s$  is equivalent to a Stokes pulse if one considers an analogous three-level atomic system for normal STIRAP. However, our choice of pulse shape can be better understood by looking at the instantaneous eigenvalues of the system.

In the rotating wave approximation the Hamiltonian (5), in the doubly rotating frame, can be written as

$$H = \begin{bmatrix} 0 & \Omega_p(t)/2 & 0 \\ \Omega_p^*(t)/2 & \delta_c(t) & \Omega_s/2 \\ 0 & \Omega_s/2 & \delta_a(t) \end{bmatrix}, \quad (9)$$

which has the right form to possess a ‘dark’ eigenstate. Consider the instantaneous eigenvalues  $(\lambda_0, \lambda_1, \lambda_2)$ , of this Hamiltonian when the time modulated pulses are applied. If the optomechanical coupling  $G_{cb}(t)$  vanishes (i.e.  $\Omega_p(t) = 0$ ), the so-called ‘Stokes Hamiltonian’ is given by

$$H_s = \begin{bmatrix} 0 & 0 & 0 \\ 0 & \delta_c(t) & \Omega_0/2 \\ 0 & \Omega_0^*/2 & \delta_a(t) \end{bmatrix}. \quad (10)$$

This Hamiltonian acts only on the two cavity subspace, i.e. it does not involve the mechanical mode, yielding the asymptotic eigenstates  $|s_0(t = \pm\infty)\rangle$ , and  $|s_\pm(t = \pm\infty)\rangle$ , where

$$|s_+(-\infty)\rangle \simeq |N_c\rangle \rightarrow |s_+(\infty)\rangle \simeq |N_a\rangle, \quad (11)$$

$$|s_-(-\infty)\rangle \simeq |N_a\rangle \rightarrow |s_-(\infty)\rangle \simeq |N_c\rangle. \quad (12)$$

Here  $|N_a\rangle$  ( $|N_c\rangle$ ) are Fock states of the auxiliary (primary) optical cavities and the corresponding eigenvalues are

$$S_0 = 0, \quad S_\pm = \delta_a + \frac{\delta_s \pm \sqrt{\delta_s^2 + \Omega_0^2}}{2}. \quad (13)$$

The time evolution of the eigenvalues of this Stokes Hamiltonian using the pulses shown in Fig. 2(a), results in the eigenvalues  $S_\pm(t)$  crossing the eigenvalue  $S_0$  twice at  $t \sim \pm t_c$ . However, when the Gaussian coupling  $\Omega_p$  is applied, it lifts the degeneracy between  $S_0$  and  $S_+$ , resulting in an avoided crossing, which leads to population transfer. The time evolution of the phonon occupancy in the mechanical resonator,  $N_b$ , and photon occupancy in the two cavities,  $N_a$  and  $N_c$ , are shown in Fig. 2(b) for the case when initially  $(N_b, N_a, N_c) = (1, 0, 0)$ , found by solving the Schrödinger equation without considering any coupling of the system to external baths. One can see that the population is transferred with virtually 100% fidelity from the phonon  $b$ -mode to the auxiliary cavity  $a$ -mode. The population in the primary cavity  $c$ -mode, is briefly non-zero and quickly returns to vanishing occupancy, leading to a complete transfer to the auxiliary cavity mode, despite a vast difference in frequencies between the mechanical and optical modes. This method will be extended in the following to study the population dynamics in a realistic open system by coupling each mode to a thermal bath.

*In presence of damping* — In order to apply our proposed method in a realistic setup one needs to consider open quantum system dynamics. The phonon number evolution can be studied via covariance methods using

the quantum master equation, which for our model is given by

$$\begin{aligned} \dot{\rho} = & i[\rho, H] + \left\{ \kappa_a (\bar{n}_a + 1) \mathcal{D}[a_1] + \kappa_a \bar{n}_a \mathcal{D}[a_1^\dagger] \right. \\ & + \kappa_c (\bar{n}_c + 1) \mathcal{D}[c_1] + \kappa_c \bar{n}_c \mathcal{D}[c_1^\dagger] \\ & \left. + \kappa_b (\bar{n}_b + 1) \mathcal{D}[b_1] + \kappa_b \bar{n}_b \mathcal{D}[b_1^\dagger] \right\} \rho, \end{aligned} \quad (14)$$

where

$$\begin{aligned} H = & \delta_a(t) a_1^\dagger a_1 + \delta_c(t) c_1^\dagger c_1 + G_{cb}(t) (c_1^\dagger b_1 + c_1 b_1^\dagger + e^{-2i\omega_b t} \\ & c_1 b_1 + e^{2i\omega_b t} c_1^\dagger b_1^\dagger) + g_{ca} (c_1^\dagger a_1 + c_1 a_1^\dagger), \end{aligned} \quad (15)$$

and  $\mathcal{D}[A]\rho \equiv A\rho A^\dagger - 1/2\{A^\dagger A, \rho\}$ . We use the covariance approach to find the time evolution of the mean phonon number  $\langle b_1^\dagger b_1 \rangle(t)$ . For this, we solve a linear system of differential equations

$$\partial_t \langle \hat{o}_i \hat{o}_j \rangle = \text{Tr}(\dot{\rho} \hat{o}_i \hat{o}_j) = \sum_{m,n} \mu_{m,n} \langle \hat{o}_m \hat{o}_n \rangle, \quad (16)$$

where  $\hat{o}_i, \hat{o}_j, \hat{o}_m, \hat{o}_n$  are one of the operators:  $a_1^\dagger, c_1^\dagger, b_1^\dagger, a_1, c_1$  and  $b_1$ ; and  $\mu_{m,n}$  are the corresponding coefficients. Solving these one can determine the mean values of all the time-dependent second-order moments:  $\langle a_1^\dagger a_1 \rangle, \langle c_1^\dagger c_1 \rangle, \langle b_1^\dagger b_1 \rangle, \langle a_1^\dagger c_1 \rangle, \langle a_1^\dagger b_1 \rangle, \langle c_1^\dagger b_1 \rangle, \langle c_1 b_1 \rangle, \langle a_1^\dagger b_1^\dagger \rangle, \langle c_1^\dagger a_1^\dagger \rangle, \langle b_1^\dagger c_1^\dagger \rangle$  and  $\langle a_1^\dagger a_1^\dagger \rangle$ . In the following, we will consider an initial state of the system where only the  $b$ -mode is occupied, e.g.  $\langle b_1^\dagger b_1 \rangle(t=0)$  is nonzero. We will consider that at  $t=0$ , all the other second-order moments vanish. In particular the initial thermal occupations of the optical cavities at room temperatures is assumed to be vanishingly small.

Using this approach, we plot the unitary evolution of the phonon occupation,  $N_b$ , for a system in the strong coupling regime with  $\Omega_0/\omega_b = 0.9$  in Fig. 3(a), without considering any damping in the system. Setting initially  $(N_b, N_a, N_c) = (10^3, 0, 0)$ , we see that one can achieve nearly perfect transfer out of the  $b$ -mode. In order to consider a realistic system, we incorporate damping in the system with  $\kappa_c/\omega_b = 0.5$ ,  $\kappa_a/\omega_b = 2$ , and  $Q_b = 10^7$ , and initially  $N_b = 10^3$ , and we observe the evolution shown in Fig. 3(b). Although the phonon occupation reduces significantly it does not reach the ground state. In Fig. 3(c) we plot the eigenspectrum and note that when the pump pulse is applied a gap opens up and it is this gap that permits the transfer. The size of this gap can be increased with larger  $\Omega_0/\omega_b$ , allowing faster transfers, but there are physical limits on how large  $\Omega_0/\omega_b$  can be. Since most of the transfer occurs during this gap we consider in the following a truncated portion of the full pulse chosen from the behaviour in the interval  $t \in \{T_{\text{start}}, T_{\text{end}}\}$ , which closely matches the temporal location of this gap. Iterating this truncated sub-pulse a number of times, as shown in Fig. 3(d), allows us to minimise the time for heating and thereby efficiently cool the mechanical mode to its ground state. In the following, we will apply this

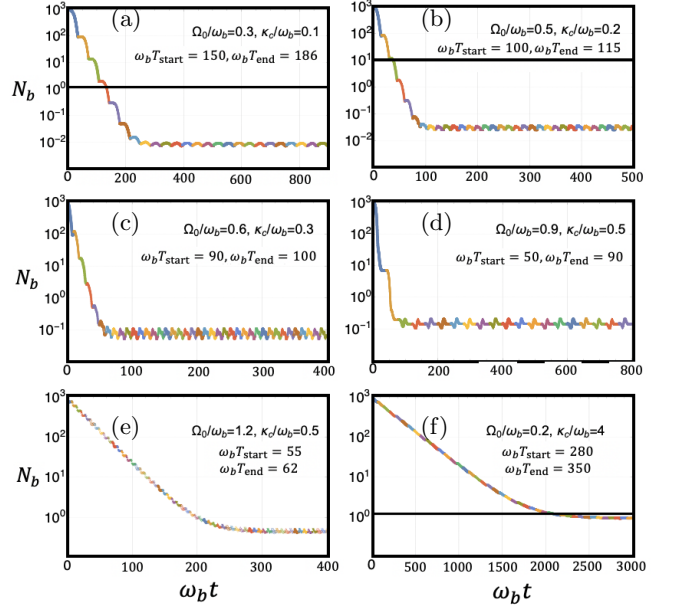


Figure 4. (Color online) Comparison between optomechanical cooling using iterated STIRAP truncated pulses and standard sideband cooling. Multicoloured curves show phonon occupancy starting from  $(N_b, N_a, N_c) = (10^3, 0, 0)$ , using STIRAP cooling for various parameters. The horizontal black solid line (wherever shown), depicts the steady-state phonon number obtained from normal sideband optomechanical cooling while in other cases normal optomechanical cooling is not possible due to instability in the system. The parameters used for each sub-graph are given in Table I. Here (a)-(e) show cases where the coupling strength  $\Omega_0/\omega_b$  gradually increases and also the resolved sideband condition becomes less valid as  $\kappa_c/\omega_b$  increases. (f) is the case for moderate coupling strength but is deep in the unresolved sideband regime. Here,  $\kappa_a/\omega_b = 2$ ,  $Q_b = 10^7$ , and  $T_{\text{start}}$  and  $T_{\text{end}}$  are the start and end time of each individual truncated sub-pulse.

method over a range of system parameters, and we will also discuss the advantages over standard optomechanical cooling.

*Comparison to standard optomechanical cooling* — In standard optomechanical cooling, a quantum cooling limit exists which is characterised by when the system finally attains a stationary state, i.e.  $d\langle o_i o_j \rangle/dt = 0$ . When working on the red side-band ( $\Delta_c = \omega_b$ ), and when the cooperativity parameter  $C \equiv 4|G|^2/(\kappa_b \kappa_c) \gg 1$ , the steady-state final mean phonon number is given by [27],

$$\begin{aligned} \langle b_1^\dagger b_1 \rangle_{\text{lim}} \simeq & \frac{4|G|^2 + \kappa_c^2}{4|G|^2(\kappa_c + \kappa_b)} \kappa_b \bar{n}_b \\ & + \frac{(4\omega_b^2 - \kappa_c^2)(8|G|^2 + \kappa_c^2) + 2\kappa_c^4}{16\omega_b^2(4\omega_b^2 + \kappa_c^2 - 16|G|^2)}, \end{aligned} \quad (17)$$

where the first term describes the cooling limit in the presence of a motional thermal environment, while the second term describes the cooling limit achieved in the case where the motional bath is the vacuum. This latter is non-zero as the cooling process itself has competing

cooling and heating rates.

In Fig. 4, we compare the reduction of the phonon occupancy achieved via iterated STIRAP pulses and standard sideband cooling in different regimes. For the parameters shown in Figs. 4(c), (d) and (e), the conditions for stability in normal sideband optomechanical cooling are violated and that cooling method fails. However, our method succeeds and one can almost reach the ground state in most cases. For the parameters shown in Figs. 4(a), (b) and (f), normal sideband cooling works, however, it is evident that our method returns better cooling in these regimes. An elaborate comparison is presented in Table II (see supplementary material) for a range of parameters from where the regimes where our method succeeds over normal sideband cooling can be easily identified. It can be seen that in the unresolved sideband regime, i.e.  $\kappa_c \gg \omega_b$ , cooling with our STIRAP pulses can be improved with higher  $\kappa_a/\omega_b$ .

*Conclusions* — Cooling of mechanical resonators remains a crucial goal in the engineering of quantum motional states of matter. Using a detuning-assisted STIRAP scheme we have shown that a cooling method exists which effectively transfers the quanta from the mechanical oscillator to an optical oscillator in a one-way fashion and operates over a broad range of parameters. Just as normal STIRAP transfer is quite robust to pulse/parameter imperfections we expect our scheme should also exhibit similar robustness.

*Acknowledgements* — We acknowledge support from the ARC Centre of Excellence for Engineered Quantum Systems CE170100009 and the Okinawa Institute of Science and Technology Graduate University.

Table I. Values of the parameters used in Figs. 2, 3 and 4. The thermal occupations  $\bar{n}_a$ ,  $\bar{n}_c$ , of the optical modes are taken to vanish, while  $\bar{n}_b$  is set equal to the mode's initial occupation, e.g.  $\bar{n}_b = 10^3$ , in Figs. 3 and 4.

Label	$\Omega_0/\omega_b$	$\omega_b\tau_{ch}$	$\kappa_\delta$	$\omega_b\tau$	$h_\delta$	$\omega_b T$	$\omega_b t_c$
2	0.1	164.99	14.05	1101.69	13.94	108.76	612.26
3	0.9	18.33	14.05	122.41	13.94	12.08	68.03
4(a)	0.3	54.99	14.05	367.23	13.94	36.25	204.08
4(b)	0.5	32.99	14.05	220.34	13.94	21.75	122.45
4(c)	0.6	27.49	14.05	183.62	13.94	18.13	102.04
4(d)	0.9	18.33	14.05	122.41	13.94	12.08	68.03
4(e)	1.2	13.74	14.05	91.81	13.94	9.06	51.02
4(f)	0.2	82.49	14.05	550.85	13.94	54.38	306.13

- [2] M. Aspelmeyer, T. J. Kippenberg, and F. Marquardt, Rev. Mod. Phys. **86**, 1391 (2014).
- [3] K. Stannigel, P. Komar, S. Habraken, S. Bennett, M. D. Lukin, P. Zoller, and P. Rabl, Phys. Rev. Lett. **109**, 013603 (2012).
- [4] A. Schliesser, P. Del'Haye, N. Nooshi, K. Vahala, and T. Kippenberg, Phys. Rev. Lett. **97**, 243905 (2006).
- [5] R. Peterson, T. Purdy, N. Kampel, R. Andrews, P.-L. Yu, K. Lehnert, and C. Regal, Phys. Rev. Lett. **116**, 063601 (2016).
- [6] T. Weiss and A. Nunnenkamp, Phys. Rev. A **88**, 023850 (2013).
- [7] M.-Y. Yan, H.-K. Li, Y.-C. Liu, W.-L. Jin, and Y.-F. Xiao, Phys. Rev. A **88**, 023802 (2013).
- [8] S. Mancini, D. Vitali, and P. Tombesi, Phys. Rev. Lett. **80**, 688 (1998).
- [9] P.-F. Cohadon, A. Heidmann, and M. Pinard, Phys. Rev. Lett. **83**, 3174 (1999).
- [10] D. Kleckner and D. Bouwmeester, Nature **444**, 75 (2006).
- [11] T. Corbitt, C. Wipf, T. Bodiya, D. Ottaway, D. Sigg, N. Smith, S. Whitcomb, and N. Mavalvala, Phys. Rev. Lett. **99**, 160801 (2007).
- [12] M. Poggio, C. Degen, H. Mamin, and D. Rugar, Phys. Rev. Lett. **99**, 017201 (2007).
- [13] A. Nunnenkamp, K. Børkje, J. Harris, and S. Girvin, Phys. Rev. A **82**, 021806 (2010).
- [14] Z. Deng, Y. Li, M. Gao, and C. Wu, Phys. Rev. A **85**, 025804 (2012).
- [15] J. D. Teufel, T. Donner, D. Li, J. W. Harlow, M. Allman, K. Cicak, A. J. Sirois, J. D. Whittaker, K. W. Lehnert, and R. W. Simmonds, Nature **475**, 359 (2011).
- [16] M. Karuza, C. Molinelli, M. Galassi, C. Biancofiore, R. Natali, P. Tombesi, G. Di Giuseppe, and D. Vitali, New J. Phys. **14**, 095015 (2012).
- [17] J.-Q. Liao and C. K. Law, Phys. Rev. A **84**, 053838 (2011).
- [18] S. Machnes, J. Cerrillo, M. Aspelmeyer, W. Wieczorek, M. B. Plenio, and A. Retzker, Phys. Rev. Lett. **108**, 153601 (2012).
- [19] K. Xia and J. Evers, Phys. Rev. Lett. **103**, 227203 (2009).
- [20] X. Wang, S. Vinjanampathy, F. W. Strauch, and K. Jacobs, Phys. Rev. Lett. **107**, 177204 (2011).
- [21] C. Genes, D. Vitali, P. Tombesi, S. Gigan, and M. Aspelmeyer, Phys. Rev. A **77**, 033804 (2008).
- [22] F. Elste, S. Girvin, and A. Clerk, Phys. Rev. Lett. **102**, 207209 (2009).
- [23] C. Genes, H. Ritsch, and D. Vitali, Phys. Rev. A **80**, 061803 (2009).
- [24] J. B. Clark, F. Lecocq, R. W. Simmonds, J. Aumentado, and J. D. Teufel, Nature **541**, 191 (2017).
- [25] M. Asjad, S. Zippilli, and D. Vitali, Phys. Rev. A **94**, 051801 (2016).
- [26] P. Di Stefano, E. Paladino, A. D'arrigo, and G. Falci, Phys. Rev. B **91**, 224506 (2015).
- [27] D.-Y. Wang, C.-H. Bai, S. Liu, S. Zhang, and H.-F. Wang, Phys. Rev. A **98**, 023816 (2018).



# Supplemental Material for “Optomechanical cooling by STIRAP-assisted energy transfer – an alternative route towards the mechanical ground state”

Bijita Sarma and Thomas Busch

*Quantum Systems Unit, Okinawa Institute of Science and Technology Graduate University, Okinawa 904-0495, Japan*

Jason Twamley

*Centre for Engineered Quantum Systems, Department of Physics and Astronomy, Macquarie University, Sydney, New South Wales 2109, Australia*

## I. LINEARIZATION OF THE HAMILTONIAN

By separating the classical mean fields and the quantum fluctuations, the classical and quantum Langevin equations can be written as

$$\begin{aligned} (-i\Delta_a - \kappa_a)\alpha - ig_{ca}\eta + \varepsilon_s &= 0, \\ (-i\omega_b - \kappa_b)\beta - ig_{cb}|\eta|^2 &= 0, \\ (-i\Delta_c - \kappa_c)\eta - ig_{ca}\alpha - ig_{cb}\eta(\beta + \beta^*) + \varepsilon_p &= 0, \end{aligned} \tag{S1}$$

and

$$\begin{aligned} \dot{a}_1 &= (-i\Delta_a - \kappa_a)a_1 - ig_{ca}c_1 + \sqrt{2\kappa_a}a_{in}, \\ \dot{b}_1 &= (-i\omega_b - \kappa_b)b_1 - ig_{cb}(\eta^*c_1 + \eta c_1^\dagger) - ig_{cb}c_1^\dagger c_1 + \sqrt{2\kappa_b}b_{in}, \\ \dot{c}_1 &= (-i\tilde{\Delta}_c - \kappa_c)c_1 - ig_{ca}a_1 - ig_{cb}\eta(b_1 + b_1^\dagger) - ig_{cb}c_1(b_1 + b_1^\dagger) + \sqrt{2\kappa_c}c_{in}, \end{aligned} \tag{S2}$$

where  $\tilde{\Delta}_c = \Delta_c + g_{cb}(\beta + \beta^*)$  with  $\beta = -ig_{cb}|\eta|^2 / (i\omega_b + \kappa_b)$ . For the parameters we consider here,  $g_{cb}(\beta + \beta^*) \ll \Delta_c$ . Therefore it can be safely approximated that  $\tilde{\Delta}_c \approx \Delta_c$ . The mean field amplitude of the primary cavity mode,  $\eta$  is given by

$$\eta = \frac{\varepsilon_p(i\Delta_a + \kappa_a) - ig_{ca}\varepsilon_s}{g_{ca}^2 + (i\Delta_c + \kappa_c)(i\Delta_a + \kappa_a)}. \tag{S3}$$

In the quantum Langevin equations, for strong drives, the product of the fluctuation terms,  $ig_{cb}c_1^\dagger c_1$  and  $ig_{cb}c_1(b_1 + b_1^\dagger)$ , can be considered as very small in comparison to the other terms, and hence been neglected. Thus the linearized Hamiltonian is obtained as

$$H_{\text{lin}} = \Delta_a a_1^\dagger a_1 + \Delta_c c_1^\dagger c_1 + \omega_b b_1^\dagger b_1 + G_{cb}(c_1 + c_1^\dagger)(b_1 + b_1^\dagger) + g_{ca}(c_1^\dagger a_1 + c_1 a_1^\dagger), \tag{S4}$$

where  $G_{cb} = \eta g_{cb}$  is the coherent-driving-enhanced linearized optomechanical coupling strength.

## II. DYNAMICAL EQUATIONS FOR THE SECOND-ORDER MOMENTS

The ordinary differential equations for the time evolution of the second-order moments can be obtained from the master equation as given below. In their derivation we do not make the rotating wave approximation and we neglect

terms proportional to the time derivatives of the modulated detunings and drive strengths.

$$\begin{aligned}
\partial_t \langle a_1^\dagger a_1 \rangle &= ig_{ca}(\langle c_1^\dagger a_1 \rangle - \langle a_1^\dagger c_1 \rangle) - \kappa_a(\bar{n}_a + 1)\langle a_1^\dagger a_1 \rangle + \kappa_a \bar{n}_a(1 + \langle a_1^\dagger a_1 \rangle), \\
\partial_t \langle c_1^\dagger c_1 \rangle &= ig_{ca}(\langle a_1^\dagger c_1 \rangle - \langle c_1^\dagger a_1 \rangle) + iG_{cb}(\langle b_1^\dagger c_1 \rangle - \langle c_1^\dagger b_1 \rangle) + iG_{cb}e^{-2i\omega_b t}\langle c_1 b_1 \rangle - iG_{cb}e^{2i\omega_b t}\langle c_1^\dagger b_1^\dagger \rangle \\
&\quad - \kappa_c(\bar{n}_c + 1)\langle c_1^\dagger c_1 \rangle + \kappa_c \bar{n}_c(1 + \langle c_1^\dagger c_1 \rangle), \\
\partial_t \langle b_1^\dagger b_1 \rangle &= -iG_{cb}(\langle b_1^\dagger c_1 \rangle - \langle c_1^\dagger b_1 \rangle) + iG_{cb}e^{-2i\omega_b t}\langle c_1 b_1 \rangle - iG_{cb}e^{2i\omega_b t}\langle c_1^\dagger b_1^\dagger \rangle - \kappa_b(\bar{n}_b + 1)\langle b_1^\dagger b_1 \rangle \\
&\quad + \kappa_b \bar{n}_b(1 + \langle b_1^\dagger b_1 \rangle), \\
\partial_t \langle a_1^\dagger c_1 \rangle &= i\delta_a \langle a_1^\dagger c_1 \rangle - i\delta_c \langle c_1 a_1^\dagger \rangle + ig_{ca}(\langle c_1^\dagger c_1 \rangle - \langle a_1^\dagger a_1 \rangle) - iG_{cb}\langle b_1 a_1^\dagger \rangle - iG_{cb}e^{2i\omega_b t}\langle a_1^\dagger b_1^\dagger \rangle - (\kappa_a/2)(\bar{n}_a + 1)\langle a_1^\dagger c_1 \rangle \\
&\quad + (\kappa_a/2)\bar{n}_a \langle c_1 a_1^\dagger \rangle - (\kappa_c/2)(\bar{n}_c + 1)\langle a_1^\dagger c_1 \rangle + (\kappa_c/2)\bar{n}_c \langle c_1 a_1^\dagger \rangle, \\
\partial_t \langle a_1^\dagger b_1 \rangle &= i\delta_a \langle a_1^\dagger b_1 \rangle + ig_{ca}\langle c_1^\dagger b_1 \rangle - iG_{cb}\langle c_1 a_1^\dagger \rangle - iG_{cb}e^{2i\omega_b t}\langle a_1^\dagger c_1^\dagger \rangle - (\kappa_a/2)(\bar{n}_a + 1)\langle a_1^\dagger b_1 \rangle + (\kappa_a/2)\bar{n}_a \langle a_1^\dagger b_1 \rangle \\
&\quad - (\kappa_b/2)(\bar{n}_b + 1)\langle a_1^\dagger b_1 \rangle + (\kappa_b/2)\bar{n}_b \langle a_1^\dagger b_1 \rangle, \\
\partial_t \langle c_1^\dagger b_1 \rangle &= i\delta_c \langle c_1^\dagger b_1 \rangle + ig_{ca}\langle a_1^\dagger b_1 \rangle + iG_{cb}(\langle b_1^\dagger b_1 \rangle - \langle c_1^\dagger c_1 \rangle) + iG_{cb}e^{-2i\omega_b t}\langle b_1 b_1 \rangle - iG_{cb}e^{2i\omega_b t}\langle c_1^\dagger c_1^\dagger \rangle \\
&\quad - (\kappa_b/2)(\bar{n}_b + 1)\langle c_1^\dagger b_1 \rangle + (\kappa_b/2)\bar{n}_b \langle c_1^\dagger b_1 \rangle - (\kappa_c/2)(\bar{n}_c + 1)\langle c_1^\dagger b_1 \rangle + (\kappa_c/2)\bar{n}_c \langle c_1^\dagger b_1 \rangle, \\
\partial_t \langle b_1 b_1 \rangle &= -2iG_{cb}\langle b_1 c_1 \rangle - 2iG_{cb}e^{2i\omega_b t}\langle c_1^\dagger b_1 \rangle + \kappa_b(\bar{n}_b + 1)\langle b_1 b_1 \rangle + \kappa_b \bar{n}_b \langle b_1 b_1 \rangle, \\
\partial_t \langle c_1 b_1 \rangle &= -i\delta_c \langle b_1 c_1 \rangle - iG_{cb}(\langle c_1 c_1 \rangle + \langle b_1 b_1 \rangle) - ig_{ca}\langle a_1 b_1 \rangle - (\kappa_b/2)(\bar{n}_b + 1)\langle b_1 c_1 \rangle + (\kappa_b/2)\bar{n}_b \langle b_1 c_1 \rangle \\
&\quad - iG_{cb}e^{2i\omega_b t}(\langle c_1^\dagger c_1 \rangle + \langle b_1^\dagger b_1 \rangle + 1) - (\kappa_c/2)(\bar{n}_c + 1)\langle b_1 c_1 \rangle + (\kappa_c/2)\bar{n}_c \langle b_1 c_1 \rangle, \\
\partial_t \langle a_1^\dagger c_1^\dagger \rangle &= i(\delta_a + \delta_c)\langle a_1^\dagger c_1^\dagger \rangle + g_{ca}(\langle c_1^\dagger c_1^\dagger \rangle + \langle a_1^\dagger a_1^\dagger \rangle) + G_{cb}\langle a_1^\dagger b_1^\dagger \rangle + G_{cb}e^{-2i\omega_b t}\langle a_1^\dagger b_1 \rangle - (\kappa_a/2)(\bar{n}_a + 1)\langle a_1^\dagger c_1^\dagger \rangle \\
&\quad + (\kappa_a/2)\bar{n}_a \langle a_1^\dagger c_1^\dagger \rangle - (\kappa_c/2)(\bar{n}_c + 1)\langle a_1^\dagger c_1^\dagger \rangle + (\kappa_c/2)\bar{n}_c \langle a_1^\dagger c_1^\dagger \rangle, \\
\partial_t \langle a_1^\dagger b_1^\dagger \rangle &= i\delta_a \langle a_1^\dagger b_1^\dagger \rangle + ig_{ca}\langle c_1^\dagger b_1^\dagger \rangle + iG_{cb}\langle a_1^\dagger c_1^\dagger \rangle + iG_{cb}e^{-2i\omega_b t}\langle a_1^\dagger c_1 \rangle - (\kappa_a/2)(\bar{n}_a + 1)\langle a_1^\dagger b_1^\dagger \rangle + (\kappa_a/2)\bar{n}_a \langle a_1^\dagger b_1^\dagger \rangle \\
&\quad - (\kappa_b/2)(\bar{n}_b + 1)\langle a_1^\dagger b_1^\dagger \rangle + (\kappa_b/2)\bar{n}_b \langle a_1^\dagger b_1^\dagger \rangle, \\
\partial_t \langle c_1^\dagger c_1^\dagger \rangle &= 2i\delta_c \langle c_1^\dagger c_1^\dagger \rangle + 2ig_{ca}\langle a_1^\dagger c_1^\dagger \rangle + 2iG_{cb}\langle b_1^\dagger c_1^\dagger \rangle + 2iG_{cb}e^{-2i\omega_b t}\langle c_1^\dagger b_1 \rangle + \kappa_c(\bar{n}_c + 1)\langle c_1^\dagger c_1^\dagger \rangle + \kappa_c \bar{n}_c \langle c_1^\dagger c_1^\dagger \rangle, \\
\partial_t \langle a_1^\dagger a_1^\dagger \rangle &= 2i\delta_a \langle a_1^\dagger a_1^\dagger \rangle + 2ig_{ca}\langle a_1^\dagger c_1^\dagger \rangle + \kappa_a(\bar{n}_a + 1)\langle a_1^\dagger a_1^\dagger \rangle + \kappa_a \bar{n}_a \langle a_1^\dagger a_1^\dagger \rangle.
\end{aligned} \tag{S5}$$

These equations can be solved to obtain the values of second order moments with respect to time.

### III. COMPARISON OF NORMAL COOLING AND STIRAP-COOLING

Table II. Comparison of steady-state phonon number calculated for normal cooling  $N_{min}^{NC}$ , and the minimal phonon number obtained using the iterated STIRAP-cooling method  $N_{min}^{SC}$ , for a variety of parameters. Here,  $\omega_b T_{start}$  and  $\omega_b T_{end}$  are the start and end time of each pulse which have been found to achieve the optimal cooling in each case. The shading is to assist the reader. We observe that STIRAP cooling succeeds in all cases and in some cases reaches lower final phonon occupations.

$G/\omega_b$	$\kappa_c/\omega_b$	$\kappa_a/\omega_b$	$Q_b$	$\omega_b T_{start}$	$\omega_b T_{end}$	$N_{min}^{NC}$	$N_{min}^{SC}$
0.02	0.05	0.01	$10^5$	3000	3180	0.51	2.11
0.02	0.05	2	$10^5$	3000	3180	0.51	1.98
0.02	0.05	0.01	$10^7$	3000	3180	0.005	0.021
0.02	0.05	2	$10^7$	3000	3180	0.005	0.020
0.1	0.1	0.01	$10^5$	500	600	0.13	0.52
0.1	0.1	2	$10^5$	500	600	0.13	0.39
0.1	0.1	0.01	$10^7$	500	600	0.0070	0.0077
0.1	0.1	2	$10^7$	500	600	0.0070	0.0058
0.3	0.1	0.01	$10^5$	150	186	0.173	0.442
0.3	0.1	2	$10^5$	150	186	0.173	0.219
0.3	0.1	0.01	$10^7$	150	186	0.071	0.016
0.3	0.1	2	$10^7$	150	186	0.071	0.008
0.5	0.2	0.01	$10^5$	100	115	12.679	0.184
0.5	0.2	2	$10^5$	100	115	12.679	0.114
0.5	0.2	0.01	$10^7$	100	115	12.628	0.046
0.5	0.2	2	$10^7$	100	115	12.628	0.030
0.6	0.3	0.01	$10^5$	90	100	unstable	0.179
0.6	0.3	2	$10^5$	90	100	unstable	0.136
0.6	0.3	0.01	$10^7$	90	100	unstable	0.097
0.6	0.3	2	$10^7$	90	100	unstable	0.080
0.9	0.5	0.01	$10^5$	50	90	unstable	0.300
0.9	0.5	2	$10^5$	50	90	unstable	0.266
0.9	0.5	0.01	$10^7$	50	90	unstable	0.161
0.9	0.5	2	$10^7$	50	90	unstable	0.149
1.2	0.5	0.01	$10^5$	55	62	unstable	1.574
1.2	0.5	2	$10^5$	55	62	unstable	0.717
1.2	0.5	0.01	$10^7$	55	62	unstable	0.441
1.2	0.5	2	$10^7$	55	62	unstable	0.451
1.5	0.5	0.01	$10^5$	44	51	unstable	1.574
1.5	0.5	2	$10^5$	44	51	unstable	1.44
1.5	0.5	0.01	$10^7$	44	51	unstable	1.143
1.5	0.5	2	$10^7$	44	51	unstable	1.03
0.2	4	0.01	$10^5$	280	350	1.273	3.512
0.2	4	2	$10^5$	280	350	1.273	3.46
0.2	4	0.01	$10^7$	280	350	1.023	0.953
0.2	4	2	$10^7$	280	350	1.023	0.940
0.5	10	0.01	$10^5$	100	150	6.480	10.09
0.5	10	2	$10^5$	100	150	6.480	9.91
0.5	10	0.01	$10^7$	100	150	6.381	5.37
0.5	10	2	$10^7$	100	150	6.381	5.277